

## Electron Scattering at Dislocations in $\text{LaAlO}_3/\text{SrTiO}_3$ Interfaces

S. Thiel,<sup>1</sup> C. W. Schneider,<sup>1</sup> L. Fitting Kourkoutis,<sup>2</sup> D. A. Muller,<sup>2</sup> N. Reyren,<sup>3</sup> A. D. Caviglia,<sup>3</sup> S. Gariglio,<sup>3</sup>  
J.-M. Triscone,<sup>3</sup> and J. Mannhart<sup>1,\*</sup>

<sup>1</sup>*Experimental Physics VI, EKM, University of Augsburg, Germany*

<sup>2</sup>*School of Applied and Engineering Physics, Cornell University, Ithaca, New York, USA*

<sup>3</sup>*Département de Physique de la Matière Condensée, University of Geneva, Switzerland*

(Received 1 July 2008; published 30 January 2009)

We report experimental investigations of the effects of microstructural defects and of disorder on the properties of 2D electron gases at oxide interfaces. The cross section for scattering of electrons at dislocations in  $\text{LaAlO}_3/\text{SrTiO}_3$  interfaces has been measured and found to equal  $\approx 5$  nm. Our experiments reveal that the transport properties of these electron gases are strongly influenced by scattering at dislocation cores.

DOI: 10.1103/PhysRevLett.102.046809

PACS numbers: 73.40.-c

At interfaces between insulating oxides, mobile electron gases can be generated. Discovered in  $\text{LaAlO}_3/\text{SrTiO}_3$  heterostructures [1], their existence has also been established at  $\text{LaAlO}_3/\text{SrTiO}_3$  (LAO/STO) [2],  $\text{KTaO}_3/\text{SrTiO}_3$  [3], and  $\text{LaVO}_3/\text{SrTiO}_3$  (LVO/STO) [4] interfaces. At the interface between the band insulators LAO and STO, a system introduced by Ohtomo and Hwang [2], magnetism [5] and superconductivity [6] have been reported. With gate fields applied in field effect transistor configurations, the conductivity of the LAO/STO interface can be tuned through a metal-insulator phase transition [7].

These exciting properties have led to numerous studies which identified three parameters to control the behavior of such interfaces for STO-based samples. First, oxygen defects can completely dominate the properties of the heterostructures. In STO-based samples that are grown at low oxygen pressure ( $p(\text{O}_2) \leq 10^{-6}$  mbar), the STO is reduced and oxygen defects dope the interface to electron densities as high as  $10^{16}$ – $10^{17}$   $\text{cm}^{-2}$  [5,8]. Second, for LAO/STO and LVO/STO heterostructures grown at high oxygen pressure, the thicknesses of the LAO and LVO layers are controlling parameters: the interface is conducting only if the LAO and LVO thicknesses exceed 3 and 4 unit cells (uc), respectively [4,7]. Third, conductivity is only achieved if the STO is terminated by a  $\text{TiO}_2$  plane.

In this Letter, we report on experiments in which we have incorporated well-defined defects into the interfaces to explore their influence on the properties of the electron gases. These experiments show that besides LAO thickness, oxygen vacancies, and substrate termination, scattering at dislocation cores is an important parameter in controlling the electron gas properties. To control the defect density, we altered the microstructure of the interface by adding individual grain boundaries using the bicrystal technology.

In the bicrystal process applied to generate the grain boundaries in the LAO film, LAO is epitaxially grown on nominally undoped STO bicrystals that contain the bound-

ary of the desired misorientation. Such grain boundaries have been analyzed in great detail in the literature ([9], and references therein). As the LAO films grow epitaxially on the STO bicrystals, the STO boundaries are replicated in the LAO films. Thereby, grain boundaries are obtained that cross the LAO and STO layers as well as the LAO/STO interfaces. We note that due to the kinetics involved in the epitaxial growth, the structural defects associated with the boundaries in the LAO are expected to be far further from thermodynamic equilibrium than the ones in the STO bicrystals [10].

The STO bicrystals used are commercially available, (001) oriented substrates containing [001]-tilt boundaries [11,12]. They were  $\text{TiO}_2$ -terminated by etching in a buffered HF-solution [13] and annealing [14]. As AFM imaging revealed, the etching did not create trenches at the boundaries. The LAO layers were deposited by pulsed laser deposition (PLD) as described in Ref. [15]. Several 5–20  $\mu\text{m}$  wide and 20–30  $\mu\text{m}$  long lines allow four-point measurements of the bicrystal boundary and of the adjacent grains. In a second experiment, LAO layers were deposited on single-crystalline STO substrates grown by the floating-zone method [16], which are known to contain more dislocations than the crystals grown by the Verneuil method. For scanning transmission electron microscopy (STEM) studies, unpatterned samples were capped with a 5 nm thick protection layer of amorphous  $\text{Al}_2\text{O}_3$ . Electron transparent samples for plan view analyses were prepared by wedge polishing followed by low energy ion milling of the backside of the samples.

A characteristic force microscopy (AFM) image in the boundary region of a bicrystalline sample is shown in Fig. 1. A smooth surface with a step-and-terrace structure originating from the unavoidable substrate miscut is observed on both sides of the boundary. The transition from the step-and-terrace system of one crystal to the other therefore causes surface steps to occur locally at the interface. These steps are typically 1 uc high, but may occa-

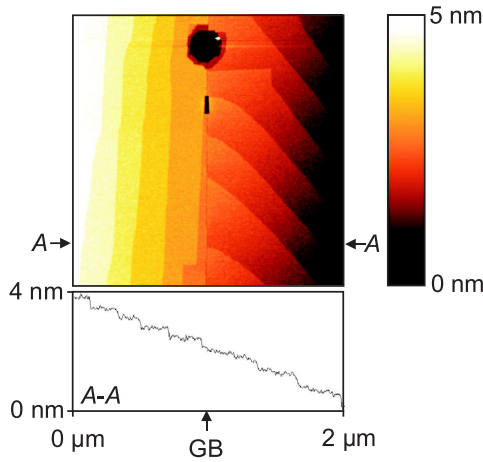


FIG. 1 (color online). Topographic AFM image and line scan of a 10 uc thick LAO film on a 4° STO bicrystal, showing the grain boundary (GB). The scan size is  $2 \times 2 \mu\text{m}^2$ .

sionally reach a height of 2–3 uc. In a few percent of the boundary length, holes may be found (Fig. 1, top) which are not visible prior to the etching.

Annular dark field (ADF) STEM images of a 4° and a 45° [001]-tilt boundary are shown in Fig. 2. Here, the samples are viewed along the [001] direction, parallel to the normals of the conducting interfaces. The tilt angles determined from the lattice fringes are  $4.2^\circ \pm 0.1^\circ$  and  $45.2^\circ \pm 0.1^\circ$ , in the two respective cases. Uniformly

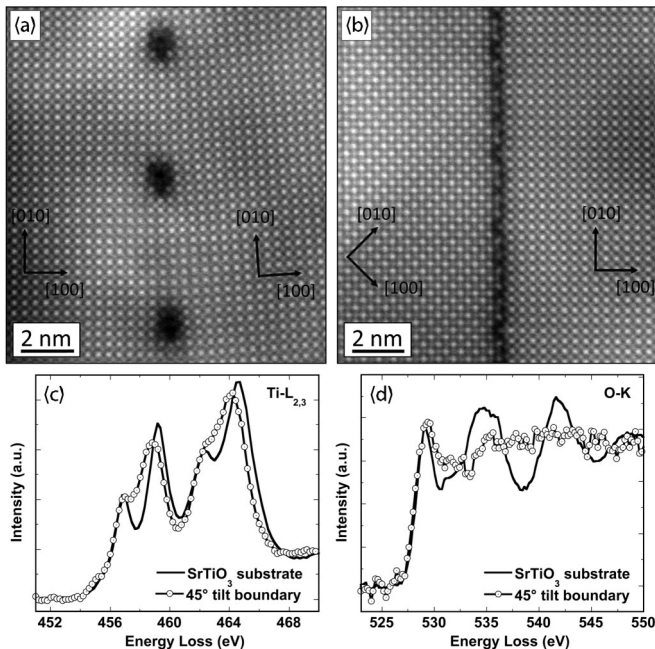


FIG. 2. High angle annular dark field STEM images of (a) 4° and (b) 45° [001]-tilt boundaries in samples of 5 uc thick LAO grown on the STO bicrystals and capped with 5 nm of  $\text{Al}_2\text{O}_3$ . (c) Ti- $L_{2,3}$  and (d) O-K electron energy loss spectra measured at the 45° tilt boundary and the STO substrate.

spaced edge dislocations are found at the 4.2° tilt boundary with an average spacing of  $(5.2 \pm 0.1)$  nm, which is in good agreement with the value of 5.3 nm determined from the tilt angle through Frank's formula [17]. As the tilt angle is increased, the spacing between dislocations decreases, and the cores merge. At the 45° tilt boundary, the boundary forms a continuous layer with a distorted structure, visible as a line of reduced ADF intensity. The chemistry of these tilt boundaries was measured on the atomic scale using electron energy loss spectroscopy (EELS). Ti- $L_{2,3}$  and O-K EELS spectra recorded in bulk STO and at the 45° tilt boundary are shown in Figs. 2(c) and 2(d). Significant changes in the near edge structure on and off the dislocation core were observed for both, the Ti-L [Fig. 2(c)] and the O-K [Fig. 2(d)] edges, suggesting a reduction of the Ti valence from 4+ in bulk STO and Sr-deficiency in the dislocation cores [18]. Obviously, the microstructure and composition in the dislocations differ significantly from the undisturbed LAO/STO interface. Therefore, in case the dislocation cores act locally on the electron gas, a scattering cross section of the core diameter ( $\approx 1$  nm) would result.

In each single crystal region (grain) of the bicrystals, the samples showed the standard transport characteristics reported before for single-crystalline samples [7]. To investigate whether the uc steps and their occasional bunching affect the transport properties, a set of samples was fabricated in which the orientation of the measurement bridges with respect to the steps was varied. No variation of the bridge resistance beyond the standard scatter ( $\approx 10\%$ ) was observed, and we conclude that the steps do not significantly influence the interface conductivity. The electron gases thus couple across steps that are one, possibly two, or even three uc high.

The transport properties across the boundaries differ from those of the grains. While the electron gas in the grains always shows Ohmic  $IV$  characteristics, Ohmic as well as nonlinear  $IV$  characteristics have been measured for the boundaries [Fig. 3(a)]. The conductivities of the electron gases straddling the boundaries are very low at

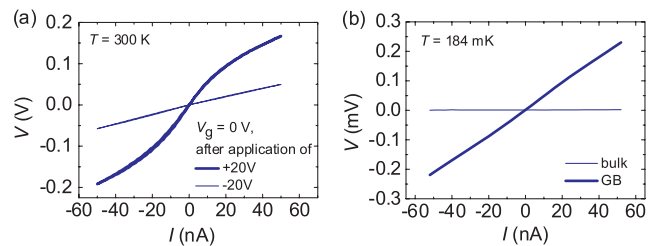


FIG. 3 (color online). (a)  $IV$  characteristics of a 2° boundary measured at  $T = 300$  K with no gate voltage applied. These characteristics can be changed by applying gate voltages of  $\pm 20$  V and remain altered even when these voltages are switched off. (b)  $IV$  characteristics of a 2° sample measured at  $T = 184$  mK across the boundary and in the adjacent grain.

large angles (Fig. 4). In the low angle regime, the conductivity increases rapidly at  $\approx 2^\circ$ , reaching values as high as  $10^2/\Omega\text{ m}$  and  $3 \times 10^{-1}/\Omega\text{ m}$  at 4 and 300 K, respectively, as obtained by measuring the resistance of the bridge crossing the boundary and subtracting the intragrain resistance of the bridge, derived from adjacent reference bridges. To investigate whether the small boundary conductivity is associated with the oxygen pressure used during deposition, a  $2^\circ$  sample was grown with  $p(\text{O}_2)$  increased by a factor of 10 to  $5 \times 10^{-4}$  mbar. The boundary conductivity of this sample equals  $2 \times 10^{-3}/\Omega\text{ m}$  and  $7 \times 10^{-3}/\Omega\text{ m}$  at 4 and 300 K, respectively, and is therefore comparable to the conductivity of the standard bicrystals (Fig. 4). To measure the boundary characteristics without grain contribution, one sample was cooled to  $T < 200$  mK [Fig. 3(b)] so that the electron gas of the grains is superconducting [19]. The resistance of the measurement bridge crossing the boundary,  $4650 \Omega$ , corresponding to a conductivity of  $\approx 10/\Omega\text{ m}$ , is therefore caused by the boundary alone. The high boundary resistance would result in a minute Josephson current of  $< 10$  nA at  $T = 0$  K which, at 180 mK, is suppressed by thermal fluctuations.

Ascribing an electronic width of  $\approx 5$  nm to the boundaries (see below), the conductivity of the  $2^\circ$  boundary is at least 3 orders of magnitude smaller than that of the neighboring grains. An increase of the boundary angle by only one degree reduces the conductivity to  $\approx 10^{-4}$ – $10^{-5}/\Omega\text{ m}$  at 300 K (8–9 orders smaller than that of the grains). For larger angles, the boundary resistance exceeds the measurement limit.

The temperature dependence of the resistance of the grains and of the  $2^\circ$  boundary differ significantly. Cooling through 40 K, the resistance of the boundaries,

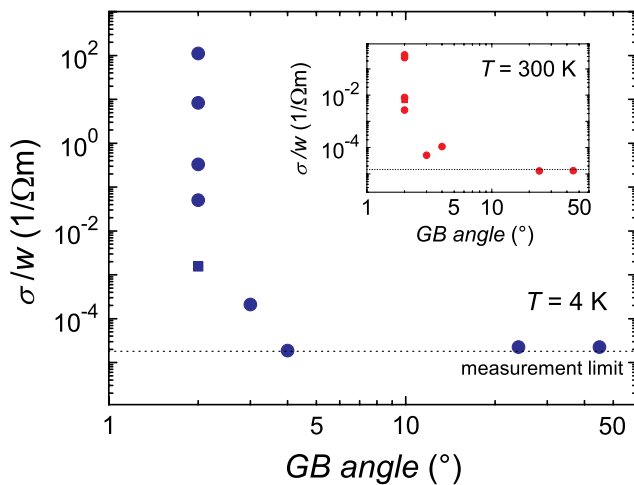


FIG. 4 (color online). Conductivity per GB width as a function of the GB angle at  $T = 4$  K. The values were obtained from the slope of  $IV$  curves at  $V = 0$  V. Inset: measurement at 300 K. The data points shown as filled squares originate from the sample grown at a higher  $p(\text{O}_2) = 5 \times 10^{-4}$  mbar as compared to the standard  $p(\text{O}_2) = 4 \times 10^{-5}$  mbar.

but not of the grains, passes through a minimum. On warming, the grain boundary resistance develops a maximum at  $\approx 70$  K; some samples generate a second one at  $\approx 230$  K [15]. While none of the grains showed any of these maxima, similar maxima have been observed in single-crystalline samples grown under different conditions [20,21].

The system is remarkably sensitive to electric gate fields. We used a field effect transistor configuration where the electric field is applied across the substrate. Although the substrates are 1 mm thick, gate voltages,  $V_g$ , of only 10–20 V change the characteristics of the electron gas at the grain boundary. As shown in Fig. 3(a),  $V_g = -20$  V, enhances the conductivity and causes a linear  $IV$  behavior. During the application of gate voltages, the gate currents were smaller than 5 nA. Reminiscent of the hysteretic field effects of electron gases reported in [7], these characteristics remain altered for hours when the gate voltage is removed. The original characteristics are recovered by applying a gate voltage pulse of opposite polarity.

To explore whether the observed behavior of the electron gas in presence of dislocations and grain boundaries is a general property of the interface electron gases, we measured the properties of interfaces grown on zone-melted STO single crystals with a very high density of edge dislocations. The LAO/STO interfaces grown on these crystals generate conducting electron gases, yet their conductivities and mobilities are 1 order of magnitude smaller than that of standard samples (see [15]).

All these results provide evidence that low angle boundaries drastically reduce the conductivity of the electron gas at the LAO/STO interface. What is the origin of this behavior?

A first candidate to depress the conductivity is the occasional presence of unit-cell steps at the boundaries. Yet, these steps cannot be the origin. Even if the current could not cross the steps, the conductance of current paths in the step-free areas would exceed the measured conductance by orders of magnitude. Further, the surfaces of the flux-grown and zone-melted STO crystals are equally flat. It would be hard to understand why the conductivities differ so much.

We therefore conclude that the 2D conductivity is reduced by edge dislocations. The measured dependence of the boundary conductance on the boundary angle can only be accounted for if each dislocation is a scattering center with a cross section of  $\approx 5$  nm. The data therefore suggest that the dislocations generate insulating disks of diameter  $D$  around their cores. This model yields for very small GB angles a strong decrease of the boundary conductivity with increasing misorientation. When the disks start to overlap at a GB angle of  $2^\circ$ – $3^\circ$  the insulating zone is continuous and the GB conductivity is vanishingly small. As will be discussed, we identify three mechanisms that could possibly be the origin of the insulating disks: mechanical strain,

changes of the local oxygen concentration, and space charges.

Edge dislocations are surrounded by stress fields. Along the grain boundary line, a dislocation causes dilatational strain in one direction, and compressive stress in the other. At first sight, it seems well possible that these lattice distortions suppress the formation of a mobile electron gas. But between two dislocations, the stress field changes sign so that locally the lattice is nominally stress free. If the conductivity was suppressed by the stress only, these stress-free areas would provide conducting paths crossing the boundaries. The high resistance of the boundaries excludes the existence of such paths. We conclude that stress and strain fields do not cause the insulating behavior.

Likewise, we exclude that possible differences in oxygen concentration between bulk and boundary are responsible for the high boundary resistance. If this was the case, the conductivity of the electron gas in the grains would be caused by oxygen defects [5,8,20]. However, samples grown under the conditions used are only conducting if the LAO layer is more than 3  $\mu\text{m}$  thick. The existence of this critical thickness and the insensitivity of the boundary properties to the oxygen pressure used during growth proves that the LAO thickness, rather than the density of oxygen vacancies in the STO, is the critical parameter for generating the mobile electron gas.

Charged dislocation cores, creating space charge regions, are understood to be the mechanism causing the resistance of grain boundaries in samples of doped bulk STO [22,23]. Trapped charges and migration of defects charge the dislocation cores. In case the dislocation cores of  $p$ -doped STO are positively charged and the cores in  $n$ -doped STO carry excess electrons, as reported, for example, in [22] and in [24], respectively, they induce charge-depleted disks at the interface. Our data provide only partial quantitative information on the charge density in the dislocation lines so that a calculation of the space charge disks in the interface cannot be provided.

Nevertheless, a comparison with the behavior of bulk,  $n$ -doped STO bicrystals reveals that the screening is likely reduced in the two-dimensional LAO/STO interfaces as compared to the bulk. In bulk doped bicrystals, the boundaries have higher conductivities than the boundaries in the LAO/STO heterostructures: in the bulk, grain boundaries with angles of  $36.8^\circ$  [24,25] have been found to be conducting, although the carrier density of these bulk samples ( $10^{17}$ – $10^{19}$   $\text{cm}^{-3}$ ) is smaller than that of the LAO/STO interfaces ( $\approx 10^{20}$   $\text{cm}^{-3}$  [6,7]).

The model of scattering by space charge layers around charged dislocations is consistent with the measured response of the grain boundary transport to gate voltages and suggests that in gate fields, additional charges migrate to or are trapped at the dislocations.

We conclude that in LAO/STO heterostructures, the dislocation cores cause insulating, charge-depleted disks in the interface with diameters of  $\approx 5$  nm. Reduction of the dislocation density will enhance the interface conductivity and mobility of the electron gas, which are a function of the microstructural quality of the STO substrates and LAO films.

The authors gratefully acknowledge helpful discussions with P. Chaudhari, G. Hammerl, T. Kopp, J. Maier, C. Richter, D. G. Schlom, and A. Schmehl. This work was supported by the DFG (SFB 484), the EC (Nanoxide), the SNSF through NCCR MANEP, and the SNSF, Division II. L. F. K., D. A. M. supported by ONR EMMA MURI, CCMR (an NSF MRSEC-DMR 0520404) and Applied Materials (L. F. K.).

---

\*Corresponding author: Jochen.Mannhart@Physik.Uni-Augsburg.de

- [1] A. Ohtomo *et al.*, Nature (London) **419**, 378 (2002).
- [2] A. Ohtomo and H. Y. Hwang, Nature (London) **427**, 423 (2004); **441**, 120 (2006).
- [3] A. S. Kalabukhov *et al.*, arXiv:07041050.
- [4] Y. Hotta *et al.*, Phys. Rev. Lett. **99**, 236805 (2007).
- [5] A. Brinkmann *et al.*, Nature Mater. **6**, 493 (2007).
- [6] N. Reyren *et al.*, Science **317**, 1196 (2007).
- [7] S. Thiel *et al.*, Science **313**, 1942 (2006).
- [8] G. Herranz *et al.*, Phys. Rev. Lett. **98**, 216803 (2007).
- [9] R. A. De Souza *et al.*, J. Appl. Phys. **97**, 053502 (2005).
- [10] J. Maier, *Festkörper-Fehler und Funktion, Prinzipien der Physikalischen Festkörperchemie* (B.G. Teubner, Stuttgart and Leipzig, 2000).
- [11] Furuuchi Chemical Corporation, Tokyo 140-0013, Japan.
- [12] Earth Chemical, Tokyo 101-0048, Japan.
- [13] M. Kawasaki *et al.*, Science **266**, 1540 (1994).
- [14] G. Koster *et al.*, Appl. Phys. Lett. **73**, 2920 (1998).
- [15] See EPAPS Document No. E-PRLTAO-102-006908 for additional information on sample preparation and further transport measurements, especially of samples grown on zone-melted SrTiO<sub>3</sub> substrates. For more information on EPAPS, see <http://www.aip.org/pubservs/epaps.html>.
- [16] CrysTec GmbH, D-12555 Berlin, Germany.
- [17] F. C. Frank, *Conference on Plastic Deformations of Crystalline Solids* (Mellon Institute, Pittsburgh, 1950), p. 150.
- [18] L. Fitting *et al.*, Ultramicroscopy **106**, 1053 (2006).
- [19] Lines placed 10  $\mu\text{m}$  away from the boundary were found to be superconducting.
- [20] W. Siemons *et al.*, Phys. Rev. B **76**, 155111 (2007).
- [21] S. Thiel *et al.* (unpublished).
- [22] Z. Zhang, W. Sigle, and M. Rühle, Phys. Rev. B **66**, 094108 (2002).
- [23] R. A. De Souza *et al.*, J. Am. Ceram. Soc. **86**, 922 (2003).
- [24] R. Shao *et al.*, Phys. Rev. Lett. **95**, 197601 (2005).
- [25] R. Shao, J. Vavro, and D. A. Bonnell, Appl. Phys. Lett. **85**, 561 (2004).